On the vapor-liquid equilibrium of attractive chain fluids with variable degree of molecular flexibility

Thijs van Westen, Thijs J. H. Vlugt, and Joachim Gross

Citation: The Journal of Chemical Physics **142**, 224504 (2015); doi: 10.1063/1.4922264
View online: http://dx.doi.org/10.1063/1.4922264
View Table of Contents: http://scitation.aip.org/content/aip/journal/jcp/142/22?ver=pdfcov
Published by the AIP Publishing

On the vapor-liquid equilibrium of attractive chain fluids with variable degree of molecular flexibility

Thijs van Westen,[1] Thijs J. H. Vlugt,[1] and Joachim Gross[2,a)]
[1]*Process and Energy Laboratory, Delft University of Technology, Leeghwaterstraat 39, 2628 CB Delft, The Netherlands*
[2]*Institut für Thermodynamik und Thermische Verfahrenstechnik, Universität Stuttgart, Pfaffenwaldring 9, 70569 Stuttgart, Germany*

(Received 17 March 2015; accepted 27 May 2015; published online 10 June 2015)

We study the isotropic (vapor and liquid) phase behavior of attractive chain fluids. Special emphasis is placed on the role of molecular flexibility, which is studied by means of a rod-coil model. Two new equations of state (EoSs) are developed for square-well- (SW) and Lennard-Jones (LJ) chain fluids. The EoSs are developed by applying the perturbation theory of Barker and Henderson (BH) to a reference fluid of hard chain molecules. The novelty of the approach is based on (1) the use of a recently developed hard-chain reference EoS that explicitly incorporates the effects of molecular flexibility, (2) the use of recent molecular simulation data for the radial distribution function of hard-chain fluids, and (3) a newly developed effective segment size, which effectively accounts for the soft repulsion between segments of LJ chains. It is shown that the effective segment size needs to be temperature-, density-, and chain-length dependent. To obtain a simplified analytical EoS, the perturbation terms are fitted by polynomials in density (SW and LJ), chain length (SW and LJ), and temperature (only for LJ). It is shown that the equations of state result in an accurate description of molecular simulation data for vapor-liquid equilibria (VLE) and isotherms of fully flexible SW- and LJ chain fluids and their mixtures. To evaluate the performance of the equations of state in describing the effects of molecular flexibility on VLE, we present new Monte Carlo simulation results for the VLE of rigid linear- and partially flexible SW- and LJ chain fluids. For SW chains, the developed EoS is in a good agreement with simulation results. For increased rigidity of the chains, both theory and simulations predict an increase of the VL density difference and a slight increase of the VL critical temperature. For LJ chains, the EoS proves incapable of reproducing part of these trends. [http://dx.doi.org/10.1063/1.4922264]

I. INTRODUCTION

Molecular-based equations of state (EoSs), where molecules are considered as chains of spherical segments have proven powerful for many practical applications.[1,2] An important step in the development of such equations of state is obtaining an accurate statistical-mechanical description of certain model fluids. Model fluids that were extensively studied, in this respect, are, for example, hard-sphere chains,[3–11] square-well (SW) chains,[12–20] Lennard-Jones (LJ) chains,[15,21–27] and, more recently, chains interacting with Mie potentials.[27,28] The theoretical description of these fluids is largely based on Wertheim's Thermodynamic Perturbation Theory (TPT).[3,4] Based on properties of a reference system of *unbonded* monomers (i.e., the EoS and cavity correlation function), TPT provides the means to calculate the Helmholtz energy for a fluid in which these monomers are connected to form chains.[5,29] As an example, applying TPT to a reference fluid of SW monomers leads to an EoS for SW-chain fluids.

A well-known artefact of TPT is that, up to first level of approximation (TPT1), it does not distinguish between chains of different flexibility constraints. While early molecular simulation studies on the subject indeed showed large similarities in the isotropic fluid phase behavior of fully flexible and rigid chains,[30] it was shown later that these conclusions are valid only for a small range in density and if the chains are sufficiently short (<5 segments).[31] Among others, it has been shown that there are large differences in the virial coefficients of rigid- and flexible chain fluids.[31–33] Although, to some extent, these large differences seem to cancel each other in the equation of state of the fluids,[30,31] it has recently been shown that the subtle differences that remain[11] need to be captured to arrive at a reliable description of phase equilibria.[34,35] In the present work, our focus is on the development of an equation of state that can describe the effects of molecular flexibility on vapor-liquid phase equilibria.

Although TPT can be extended to higher order (such as TPT2), where, in principle, the effect of molecular flexibility can be included to some extent, the extension is cumbersome since it requires the specification of higher order correlation functions of the monomeric reference fluid. For attractive chain fluids, which we aim at in this paper, these correlation functions

a)Author to whom correspondence should be addressed. Electronic mail: gross@itt.uni-stuttgart.de

are largely unavailable. In addition, if the higher correlation functions of the monomeric reference fluid would be available, such as for the case of hard repulsive chain fluids, the application of TPT2 to describe the effects of molecular flexibility would not likely be very successful.[11]

A different route to the EoS of attractive chain fluids is to treat the bonding of segments at the stage of the reference fluid. Attractive interactions between the segments of the chains are then treated as a perturbation to this reference fluid. In the present work, we use such a method to develop a perturbed-chain EoS for the isotropic fluid (vapor and liquid) phase of SW- and LJ chains. The effect of attractive interactions between the segments of the chains is treated within the framework of a second order Barker Henderson (BH) perturbation theory.[36,37] The merit of using a perturbed-chain approach lies in the fact that we are not limited to TPT for describing the bonding of segments into chains. Instead, we use a recent extension of the Liu-Hu (LH) EoS.[11,38] For fully flexible hard-chain fluids, this EoS is considerably more accurate than TPT. Moreover, the extended LH EoS[11] (referred to as LHrc EoS, where rc stands for rod-coil) explicitly accounts for the effects of (partial) intramolecular flexibility, and can thus be used to study the effect of chain flexibility on the vapor-liquid equilibrium (VLE).

Although the concept of applying the BH theory to a hard-chain reference fluid is not strictly new (see for example Refs. 18 and 39–41), a rigorous evaluation of the method by comparison to molecular simulation data of attractive chain fluids with soft repulsion (e.g., Lennard-Jones) has not yet been provided in the literature. In the present work, we show that naively applying the method to the fluid phase of LJ chains leads to unexpected deviations in calculated VLE and isotherms. In particular, we show that the conventional Barker-Henderson diameter, which serves to model the soft repulsion between LJ segments, is inadequate when applied to a fluid phase of chain molecules. A new effective diameter, which depends on temperature, chain length, and density is developed. When applied in the perturbation theory, a major improvement in the prediction of VLE and isotherms is observed. Furthermore, we show that the calculation of VLE is quite sensitive to any approximations made for describing the radial distribution function (rdf) of the hard-chain reference fluid. As an example, it is demonstrated that Chiew's PY2 approximation[42] for the hard-chain rdf results in an overestimation of the attractive contribution to the EoS, leading to a significant overestimation of vapor-liquid critical points. We show that inaccuracies of this kind can be overcome by the use of molecular simulation data for the radial distribution function.[41,43,44]

This paper is organized as follows. In Sec. II, we discuss the molecular model underlying the equations of state. After that, in Sec. III, we present the details of the MC simulations performed in this work. In Sec. IV, we lay out the perturbation theory and develop the new effective segment size for LJ chain fluids. Furthermore, the equations of state are simplified by developing analytical functions for the first and second order perturbation terms. In Sec. V, computed VLE, vapor pressure curves, and isotherms are compared to molecular simulation results obtained in this work and from the literature. Our findings are summarized in Sec. VI.

II. MOLECULAR MODEL AND INTERMOLECULAR POTENTIALS

We assume a molecule as a homo-segmented chain of m tangent spheres. We introduce molecular flexibility by arranging one part (of m_R spheres) of a chain in a rigid linear conformation (i.e., with a fixed bond angle of 180°), while the other part is freely jointed (i.e., without any angular potential). The resulting model is referred to as a rod-coil fluid. To characterize the partial rigidity of a rod-coil molecule, we use a dimensionless rigidity parameter, which is defined as the ratio of rigid bond-angles ($m_R - 2$) to total bond-angles ($m - 2$), according to

$$\chi_R = \begin{cases} \dfrac{m_R - 2}{m - 2}, & \text{for } m > 2 \\ 1, & \text{for } m \le 2 \end{cases}. \tag{1}$$

The rigidity parameter varies between zero and unity for a completely flexible- and rigid chain molecule, respectively, and serves as an input for the hard-chain reference EoS used in this work.[11]

Both, a SW- and LJ 12-6 potential are evaluated to model dispersive intermolecular interactions. The interaction energy between two segments separated by a radial distance r is thus calculated as

$$u^{SW}(r) = \begin{cases} \infty, & \text{for } r < \sigma \\ -\epsilon, & \text{for } \sigma \le r \le \lambda\sigma, \\ 0, & \text{for } r > \lambda\sigma \end{cases} \tag{2}$$

$$u^{LJ}(r) = 4\epsilon\left[\left(\frac{\sigma}{r}\right)^{12} - \left(\frac{\sigma}{r}\right)^{6}\right]. \tag{3}$$

Here, ϵ and σ are the depth of the potential well and the segment size parameter, respectively. The range of the SW interactions is set to $\lambda = 1.5$. For interactions between chains of different type i and j, the segment size parameter and depth of the potential well are approximated using the Lorentz-Berthelot combining rules, according to[45,46]

$$\sigma_{ij} = \frac{\sigma_{ii} + \sigma_{jj}}{2}, \tag{4}$$

$$\epsilon_{ij} = \sqrt{\epsilon_{ii}\epsilon_{jj}}, \tag{5}$$

where σ_{ii} and ϵ_{ii} are the potential parameters of a chain of type i. For pure component systems, these subscripts will be dropped.

III. SIMULATION DETAILS

Molecular simulations were conducted as Monte Carlo simulations in the grand-canonical (GCMC) ensemble, i.e., for a defined chemical potential μ, temperature, and volume. We performed simulations for the VLE as well as for pure-component isotherms. The molecule number N is a fluctuating quantity in GCMC simulations. For both types of simulations, we divided the N-space into windows of $\Delta N = 10$ and performed an individual GCMC simulation for each window.[47,48] Any trial move for inserting or deleting molecules beyond the dedicated interval ΔN is trivially rejected. For an efficient and even sampling of the histogram $p(N)$ within each window, we applied a transition matrix (TM)

sampling scheme and applied a TM bias function.[49] For windows of higher molecule numbers, corresponding to liquid-like densities, we applied a configurational-bias scheme[50,51] for improved statistics of molecule insertions, deletions, and reconfigurations. The volume of the system was set to $V = 2000\sigma^3$. The LJ interactions were calculated for segments belonging to different chains and for segments within the same chain separated by two or more bonds. All interactions were truncated at 4σ. Standard long-ranged tail corrections were applied.[52]

GCMC simulations require the definition of chemical potentials. For isotherms, we obtained the chemical potentials for each window from the EoS proposed in this work. The isotherms were then calculated similar to the procedure described by Shen and Errington.[48] Properties along an isotherm, such as pressure and chemical potential, are determined from histogram reweighting techniques in a post-processing step. We determined the equilibrium chemical potential for any defined molecule number $N(\mu,V,T) = \langle N\rangle$, by summing over the probability distribution $\langle N\rangle = \sum_{i=1}^{N_{\max}} p(i)\cdot i$. In doing so, our results much improved for the low density range compared to the procedure in Ref. 48.

Phase equilibria were calculated using a similar approach as for the calculation of isotherms, except that both the chemical potential μ and the temperature of the windows in N-space were estimated from the EoS described here. The values of μ and T are determined to approximately trace the vapor-liquid phase envelope. Histogram reweighting then allows the calculation of the actual phase equilibrium properties in a post processing step. The critical point is determined by applying a mixed field scaling approach.[53,54] For a more detailed description of the simulation procedure, we refer to the literature.[55]

Standard deviations of the simulation results were approximated from 3 independent simulations runs. For isothermal pressures, the standard deviation was typically lower than 0.1%. For vapor-liquid equilibria, we found deviations lower than 0.25% for pressure, lower than 0.34% for liquid density, and lower than 0.6% for vapor density. By performing the 3 independent simulation runs for different system sizes $V = \{2000\sigma^3\ 3000\sigma^3\ 4000\sigma^3\}$, we could apply a finite size scaling approximation for the critical points.[56] Typical errors due to the finite size of the system are estimated as 0.1% for the critical temperature, 2.4% for the critical density, and 0.6% for critical pressure.

IV. EQUATION OF STATE

To develop the EoS, we apply a perturbation theory.[57] In doing this, it is assumed that the rdf[57] of a fluid is mainly determined by interactions between repulsive molecular cores. Following from this argument, one can write the Helmholtz energy of a system of N molecules at absolute temperature T as a sum of a repulsive reference contribution (A_0) and an attractive perturbation contribution (A^{pert}), according to

$$\frac{A}{VkT} = a = a_0 + a^{\text{pert}}. \tag{6}$$

Here, k is Boltzmann's constant and $a = A/VkT$ is a reduced Helmholtz energy density.

Different methods have been proposed to split the intermolecular potential into a repulsive part and an attractive part.[36,37,57–59] In the present work, we use the method as originally proposed by Barker and Henderson (BH).[36,37] We thus obtain

$$u_0(r) = \begin{cases} u(r), & \text{for } r < \sigma \\ 0, & \text{for } r \geq \sigma \end{cases}, \tag{7}$$

$$u^{\text{pert}}(r) = \begin{cases} 0, & \text{for } r < \sigma \\ u(r), & \text{for } r \geq \sigma \end{cases}. \tag{8}$$

For LJ fluids, it is common to map the properties of the soft-repulsive reference fluid as defined by Eq. (7) to those of a hard-repulsive reference fluid by using an "effective" temperature-dependent segment diameter $d(T)$. The use of such an effective hard-sphere segment diameter is convenient since the properties of hard repulsive fluids are generally more readily obtained from theoretical methods than those of soft repulsive fluids. In the original BH theory, which was developed for spherical molecules, the effective segment diameter d^{BH} was calculated from the following integral:[37,57]

$$d^{\text{BH}}(T) = \int_0^{\sigma} \left(1 - \exp\left(-\frac{u(r)}{kT}\right)\right) \mathrm{d}r. \tag{9}$$

In the present work, we show that, when applied to chain fluids, the segment size resulting from this equation is too small. As a result, when used in the perturbation theory, computed VLE and isotherms are of poor quality. In Sec. IV C, we develop a simple expression for the effective segment diameter of chain fluids.

A. Reference fluid

The EoS of the hard-chain reference fluid is calculated from the sum of an ideal (id), a hard-sphere (hs), and a hard-chain (hc) contribution, according to

$$a_0 = a^{\text{id}} + a^{\text{hs}} + a^{\text{hc}}. \tag{10}$$

For a canonical N_C-component mixture, the ideal contribution to the reduced Helmholtz energy density is obtained from

$$a^{\text{id}} = \sum_i^{N_C} \rho_i \left[\ln\left(\rho_i \Lambda_i^3\right) - 1\right], \tag{11}$$

where $\rho_i = N_i/V$ is the number density of molecules of component i and Λ_i is a thermal de Broglie wavelength.

Since we will consider both, mixtures of chains with equally and non-equally sized segments, the hard-sphere contribution is obtained from the expression of Boublík[60] and Mansoori *et al.*,[61] according to

$$a^{\text{hs}} = \rho_s \frac{1}{\zeta_0}\left[\left(\frac{\zeta_2^3}{\zeta_3^2} - \zeta_0\right)\ln(1-\zeta_3) + \frac{3\zeta_1\zeta_2}{1-\zeta_3} + \frac{\zeta_2^3}{\zeta_3(1-\zeta_3)^2}\right], \tag{12}$$

where $\rho_s = \sum_i m_i\rho_i$ is the total segment density of the system and $\zeta_n = (\pi/6)\sum_i \rho_i m_i d_{ii}^n$. Please note that $\zeta_3 = \eta$, where η is the packing fraction of the system.

To calculate the hard-chain contribution, we use a recent extension[11] of the EoS of Liu and Hu[38] to rigid linear- and partially flexible chain fluids. The extended EoS (referred to as LHrc EoS) was developed to explicitly account for the effects of (partial) intramolecular flexibility, as defined by the rod-coil model from Sec. II. As in the approach of Liu and Hu, the LHrc EoS is based on a decomposition of the m-particle cavity correlation function of a chain fluid into a product of nearest- $(j, j+1)$ and next-to-nearest neighbour $(j, j+2)$ contributions. The hard-chain contribution resulting from this decomposition is written as follows:

$$a^{\mathrm{hc}} = -\sum_{i}^{N_C} \rho_i (m_i - 1) \ln y_{(i),j,j+1} - \sum_{i}^{N_C} \rho_i (m_i - 2) \ln y_{(i),j,j+2}. \tag{13}$$

The correlations between nearest- and next-to-nearest neighboring segments in a chain of type i are calculated according to the functional form as proposed by Liu and Hu,

$$\ln y_{(i),j,j+1} = \frac{(3 - a_2 + b_2 - 3c_2)\eta - (1 - a_2 - b_2 + c_2)}{2(1-\eta)} + \frac{1 - a_2 - b_2 + c_2}{2(1-\eta)^2} - (c_2 + 1)\ln(1-\eta), \tag{14}$$

$$\ln y_{(i),j,j+2} = \frac{m_i - 1}{m_i}\left[\frac{(-a_{3,i} + b_{3,i} - 3c_{3,i})\eta - (-a_{3,i} - b_{3,i} + c_{3,i})}{2(1-\eta)} + \frac{-a_{3,i} - b_{3,i} + c_{3,i}}{2(1-\eta)^2} - c_{3,i}\ln(1-\eta)\right]. \tag{15}$$

For the nearest-neighbor contribution, the LHrc EoS assumes the same model constant as obtained by Liu and Hu, i.e., $a_2 = 0.456\,96$, $b_2 = 2.103\,86$, and $c_2 = 1.755\,03$. The model constants governing the next-to-nearest neighbor contribution were correlated to molecular simulation data for the second virial coefficient of hard rod-coil fluids ($a_{3,i}$) and the pressure of hard rod-coil fluids ($b_{3,i}$ and $c_{3,i}$), by introducing the following dependence on the rigidity parameter $\chi_{\mathrm{R},i}$:[11]

$$a_{3,i} = p(1) + p(2)\chi_{\mathrm{R},i} + p(3)\chi_{\mathrm{R},i}^2 + p(4)\chi_{\mathrm{R},i}^3, \tag{16}$$

$$b_{3,i} = 3.496\,95 - 3.814\,67\chi_{\mathrm{R},i}, \tag{17}$$

$$c_{3,i} = 4.832\,07 - 1.351\,91\chi_{\mathrm{R},i}, \tag{18}$$

$$\boldsymbol{p} = (-0.747\,45,\ 0.299\,15,\ 1.087\,27,\ -0.708\,98). \tag{19}$$

It was shown that the above equations result in an accurate description of the effects of (partial) intramolecular flexibility on the equation of state. Compared to conventional EoSs, such as TPT1,[3,5] TPT2,[4,29] or GFD,[6] the LHrc EoS leads to a more reliable description of both the pressure and second virial coefficients of rigid linear, partially flexible (rod-coil), and fully flexible tangent hard-sphere chain fluids and their mixtures.[11]

B. Contribution due to attractive perturbation

To start, let us assume a pure component system of N chain molecules at a temperature T. In the framework of a second order BH theory, the contribution to the Helmholtz energy due to dispersive intermolecular attractions can then be written as a sum of a first and second order term, according to[36,37]

$$a^{\mathrm{pert}} = a_1 + a_2. \tag{20}$$

Following Barker and Henderson, we treat the first order term exactly, while the second order term is calculated based on the local compressibility approximation[36] (LCA). For simplicity, the density derivatives associated with the LCA are calculated for a constant segment size d. Although this introduces some approximation (since d as developed later in work includes a density dependence), we verified the effect is negligible compared to a "correct" application of the LCA. For pure-component systems, we obtain

$$a_1 = \frac{2\pi\rho^2}{kT}\sum_{\alpha=1}^{m}\sum_{\beta=1}^{m}\int_{\sigma}^{\infty} u(r) g_{\alpha\beta}^{\mathrm{hc}}(r) r^2 dr, \tag{21}$$

$$a_2 = -\frac{\pi\rho^2}{(kT)^2} m K_0 \frac{\partial}{\partial\rho}\left(\rho\sum_{\alpha=1}^{m}\sum_{\beta=1}^{m}\int_{\sigma}^{\infty} u^2(r) g_{\alpha\beta}^{\mathrm{hc}}(r) r^2 dr\right)_d. \tag{22}$$

Here, we have introduced the segment-segment rdf of the hard-chain reference fluid, $g_{\alpha\beta}^{\mathrm{hc}}(r, m, \chi_{\mathrm{R}}, \eta)$, which is a measure for the probability to find a segment α of chain 1 at a radial distance r from a segment β of chain 2, averaged over the positions of all other segments in the system. In the remainder, only the r-dependence of the rdf will be written explicitly.

Please note that the perturbation contributions Eqs. (21) and (22) are here written without a contribution due to interactions between segments within the same chain. In the present work, we assume the state-point dependence of the intramolecular distribution function is fully determined by the temperature. As a result, the intramolecular part of the perturbation contribution has no effect on pressure or phase equilibria and can thus be treated in the ideal-gas part of the equation of state. Although this approximation neglects the change in chain conformation that is generally observed at the vapor-liquid phase transition of chain fluids, we should note that many accurate equations of state for isotropic fluids (e.g., PC-SAFT[39]) are based on the same approximation, constituting some confidence in its application.

The isothermal compressibility of the hard-chain reference system $K_0 = kT(\partial\rho/\partial P_0)_T$ enters the equation for a_2 due to the use of the LCA. K_0 is obtained from the compressibility

factor of the hard-chain reference system $Z_0 = P_0/\rho kT$, as

$$K_0 = \left(Z_0 + \rho\left(\frac{\partial Z_0}{\partial \rho}\right)_d\right)^{-1}, \tag{23}$$

where Z_0 is calculated using the simplified version of the LHrc EoS[11] (see supplementary material[62] for details). For mixtures of chains with unequally sized segments, the use of the simplified LHrc EoS to calculate K_0 introduces some approximation since the simplified LHrc EoS implicitly assumes the Carnahan-Starling equation for the hard-sphere contribution. We verified that the effect of this approximation is negligible.

To proceed, it is convenient to introduce an averaged rdf, according to[42]

$$g^{\rm hc}(r) = \frac{1}{m^2}\sum_{\alpha=1}^{m}\sum_{\beta=1}^{m} g^{\rm hc}_{\alpha\beta}(r). \tag{24}$$

Due to the averaging, all segments in a chain are now indistinguishable. The use of an averaged rdf introduces no approximation. Upon introducing a reduced radial distance $x = r/\sigma$ and potential energy $\tilde{u}(x) = u(x\sigma)/\epsilon$, the perturbation contributions can be recast in the following dimensionless form:

$$a_1 = 2\pi\rho^2 m^2 \frac{\epsilon}{kT}\sigma^3 I_1, \tag{25}$$

$$a_2 = -\pi\rho^2 m K_0 m^2\left(\frac{\epsilon}{kT}\right)^2\sigma^3\frac{\partial}{\partial\rho}(\rho I_2)_d. \tag{26}$$

Here, we have introduced the abbreviations I_1 and I_2 for the correlation integrals. For SW chain fluids, these are obtained from the following equations:

$$I_1^{\rm SW}(m,\chi_{\rm R},\eta) = -\int_1^{\lambda} g^{\rm hc}(x\sigma)\,x^2 dx, \tag{27}$$

$$I_2^{\rm SW}(m,\chi_{\rm R},\eta) = -I_1^{\rm SW}(m,\chi_{\rm R},\eta). \tag{28}$$

For LJ chain fluids, the rdf is calculated for an effective hard-chain reference fluid of segment size d. As a results, the correlation integrals become temperature dependent,

$$I_1^{\rm LJ}(m,\chi_{\rm R},\eta,T) = \int_1^{\infty} \tilde{u}(x) g_d^{\rm hc}(x\sigma)\,x^2 dx, \tag{29}$$

$$I_2^{\rm LJ}(m,\chi_{\rm R},\eta,T) = \int_1^{\infty} \tilde{u}^2(x) g_d^{\rm hc}(x\sigma)\,x^2 dx. \tag{30}$$

We should note that in the application of the above two equations, a subtle point arises. In a correct application of the concept of an effective segment size to attractive chain fluids, the bond distance between neighbouring segments in a chain molecule should be σ. Therefore, a suitable rdf of the reference fluid would be for a fluid of hard segment diameter d and bond distance σ. Applying a rdf for chains of tangent hard spheres of diameter d and bond distance d constitutes an approximation. Although this is a commonly employed approximation,[16,28,63] its effect on calculated thermodynamic properties is difficult to assess *a priori*.

Let us now consider the calculation of the rdf of the hard-chain reference fluid. Although the rdf will clearly have some dependence on the degree of flexibility ($\chi_{\rm R}$) of the chains, we will neglect this dependence and assume the rdf of a fully flexible chain fluid can be used. This approximation seems reasonable, since the effect of intramolecular flexibility is already considered explicitly in the reference contribution to the EoS. Moreover, the approximation is convenient since the rdf of fully flexible tangent hard-sphere chain fluids can be obtained accurately from recently published MC data.[41]

In a previous study,[18] the rdf was obtained from an integral equation theory of Chiew, which was based on a Percus-Yevick closure (PY2).[42] We found that (for $m > 2$) this approximate rdf leads to systematically too high values when compared to MC simulations. To illustrate the approximation that comes with the PY2 approach, we calculated the VLE of fully flexible SW- and LJ 8-mers from the 2nd order perturbation theory detailed above, using both the rdf obtained from MC simulations and the PY2 theory. The calculations for the LJ chain fluid are based on the original BH diameter from Eq. (9). In Fig. 1, the results are compared to MC simulation results of Escobedo and de Pablo.[15] Due to the overestimation of the

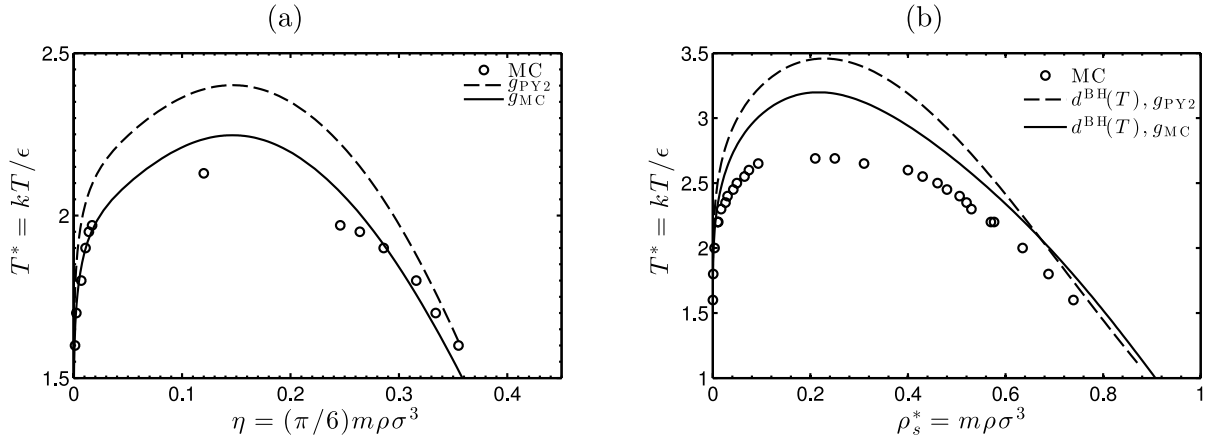

FIG. 1. The VLE of (a) a fully flexible SW 8-mer fluid and (b) a fully flexible LJ 8-mer fluid, as obtained from MC simulations[15] (symbols) and a second order Barker-Henderson perturbation theory. Theoretical results are obtained using a rdf from the PY2 theory[42] ($g_{\rm PY2}$) as input (dashed line) or a rdf from MC simulations[41] ($g_{\rm MC}$) as input (solid line). The results in (b) were obtained based on the original Barker-Henderson diameter $d^{\rm BH}(T)$ from Eq. (9). The results in this figure show that the incorporation of MC data for the rdf in the calculation of the correlation integrals improves the description of VLE. Furthermore, the results suggest that the original Barker-Henderson diameter calculated from Eq. (9) underestimates the effective segment size of the segments in LJ chain fluids.

rdf, the perturbation terms a_1 and a_2 calculated from the PY2 theory are too negative, leading to a large overestimation of the VL critical temperature and a poor prediction of vapor-liquid coexistence densities. The VLE calculated using MC data for the rdf is clearly in better agreement with the simulated phase envelope. For the SW 8-mer, good agreement with simulation data is obtained. For the LJ 8-mer, however, a significant discrepancy with the VLE as obtained from MC simulations remains. Although a perturbation theory truncated at second order will always result in an overestimation of the VL critical temperature (because density fluctuations characterizing the critical point are only partly described), the overestimation of saturated liquid densities is too pronounced to be attributed to the truncation of the perturbation expansion. Given the high accuracy of the hard-chain reference EoS,[38] the reason for the discrepancy must be sought in the perturbation terms or in the link between the hard- and soft repulsive reference systems. As the possible sources of error, we therefore identity (1) the LCA approximation used for the 2nd order perturbation term or (2) the use of the original BH diameter to describe the soft repulsion of LJ chain fluids. As the LCA approximation is known to lead to an underestimation of liquid densities at the low-temperature part of the VLE,[64] the overestimation of liquid densities that is observed in Fig. 1(b) must be caused by the use of the BH diameter. In fact, given the large overestimation of the critical temperature, the effective segment size must be underestimated.

C. New effective segment diameter for LJ chain fluids

The effective segment size should allow a mapping of the properties of a soft repulsive fluid onto those of a hard repulsive fluid. For the original BH diameter from Eq. (9), such a mapping was obtained from a scheme in which the Helmholtz energy of a system of soft repulsive spheres (with intermolecular potential defined by Eq. (7)) is expanded about the Mayer-f function of a hard-sphere reference system.[57] In this scheme, the BH diameter follows from forcing the first order term in the expansion to zero. Although, in principle, the resulting effective segment size should depend on both temperature and density,[57] the density dependence is minor for spherical molecules at typical fluid densities and was therefore not included in the original BH diameter.[37]

Evidently, to develop an effective segment size for LJ *chain* fluids, one should find a way to relate a fluid of soft *chains* to a fluid of hard *chains*. In principle, one could opt to establish such a relation by extending the above discussed expansion method to chain fluids. In the present work, however, we take a different approach by directly including simulation data in the development. To start, we consider the low-density limit, for which the effective segment size can be obtained from equating second virial coefficients,

$$B_2^{\mathrm{sc}}(T^*, m, \sigma) = B_2^{\mathrm{hc}}(m, d(T^*, m, \rho_s^* = 0)). \tag{31}$$

Here, we have introduced the dimensionless temperature $T^* = kT/\epsilon$ and the shorthand notation "sc" for "soft chain." It is important to note that, unlike the Helmholtz energy contributions in Eq. (10), the superscripts "sc" and "hc" are here meant as total contributions. For example, B_2^{hc} is the total second virial coefficient of a fluid of hard chains, which includes a hard-sphere contribution and a contribution due to chain formation.

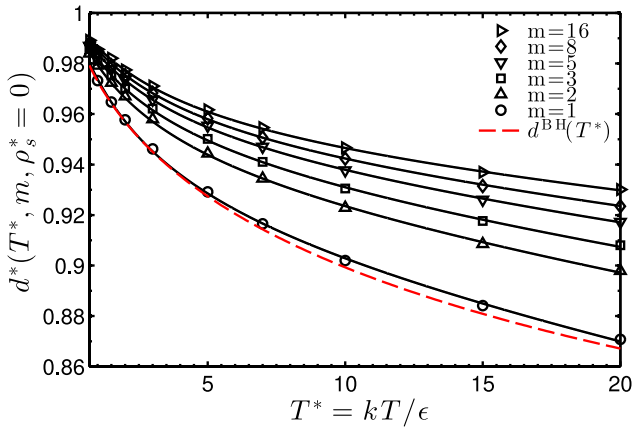

FIG. 2. The chain-length- and temperature dependence of the low-density limit of the reduced effective segment diameter $d^*(T^*, m, \rho_s^* = 0) = d(T^*, m, \rho_s^* = 0)/\sigma$ of LJ chain fluids. The symbols are obtained from equating second virial coefficients of hard- and soft-chain fluids (see Sec. IV C for details); the lines are correlation results from Eq. (32). Results for the original Barker-Henderson diameter (Eq. (9)) are also included for comparison (dashed line).

Using a MC integration method (see the Appendix for details), we calculated second virial coefficients of hard chains of length $m = \{1\ 2\ 3\ 5\ 8\ 16\}$ and $\sigma = \{0.8\ 0.85\ 0.9\ 0.95\ 0.98\ 1.0\}$. For each chain length, a power law in σ was fitted to the results. Next, we calculated second virial coefficients of soft chain fluids of the same chain lengths m at dimensionless temperatures $T^* = \{0.7\ 1.0\ 1.5\ 2.0\ 3.0\ 5.0\ 7.0\ 10.0\ 15.0\ 20.0\}$. For each temperature, we solved Eq. (31) for $d(T^*, m, \rho_s^* = 0)$, the results of which are compared to the original BH diameter in Fig. 2. As expected, the results suggest that the effective diameter of the segments in a LJ chain is larger than those of unbonded LJ spheres. For long chains, the diameter seems to approach an asymptotic value.

Given that, for $\rho_s^* < 1$, the original BH diameter $d^{\mathrm{BH}}(T^*)$ is known to give an accurate representation of the soft repulsion of LJ spheres,[57,65] the close agreement to our computed $d(T^*, m = 1, \rho_s^* = 0)$ could suggest $d(T^*, m, \rho_s^* = 0)$ is also a good representation of the effective segment size of LJ chains. Unfortunately, this is not the case. Using the GCMC method from Sec. III, we calculated isothermal pressures of soft chain fluids of length $m = \{1\ 2\ 3\ 4\}$ in the range $\rho_s^* = 0\text{-}1.0$ and $T^* = 2\text{-}20$. For simulation results, the reader is referred to the supplementary material of this work.[62] We compared simulation results to those obtained from the LHrc EoS for the hard-chain reference fluid, calculated using either the original BH diameter $d^{\mathrm{BH}}(T^*)$ or $d(T^*, m, \rho_s^* = 0)$ for the effective segment size, respectively. For all analyzed systems, the results showed indeed that the use of $d(T^*, m, \rho_s^* = 0)$ leads to a better description of the low-density regime. For larger densities, however, a significant overestimation of simulated pressures was observed. We verified that, for the chain lengths considered here, the hard-chain reference EoS is accurate to within statistical uncertainty of molecular simulations;[66,67] therefore, we conclude that the observed deviations are due to inaccuracies in the effective segment size. The effective segment size of LJ chain fluids thus needs to be density dependent.

To obtain a closed analytical function for $d(T^*, m, \rho_s^*)$, we adapt a functional form with a temperature dependence as proposed by Cotterman, Schwarz, and Prausnitz,[68] as

$$\frac{d(T^*, m, \rho_s^*)}{\sigma} = \frac{1 + A(m, \rho_s^*)T^*}{1 + B(m, \rho_s^*)T^* + C(m, \rho_s^*)T^{*2}}. \quad (32)$$

For the chain-length dependence of the coefficients A, B, and C, a functional form as proposed by Hu, Liu, and Prausnitz[10] is used,

$$A(m, \rho_s^*) = A_0(\rho_s^*) + A_1(\rho_s^*)\frac{m-1}{m} + A_2(\rho_s^*)\frac{m-1}{m}\frac{m-2}{m}, \quad (33)$$

$$B(m, \rho_s^*) = B_0(\rho_s^*) + B_1(\rho_s^*)\frac{m-1}{m} + B_2(\rho_s^*)\frac{m-1}{m}\frac{m-2}{m}, \quad (34)$$

$$C(m, \rho_s^*) = C_0(\rho_s^*) + C_1(\rho_s^*)\frac{m-1}{m} + C_2(\rho_s^*)\frac{m-1}{m}\frac{m-2}{m}. \quad (35)$$

This chain length dependence distinguishes between nearest- and next-nearest neighbor effects in chain molecules. Moreover, it is capable of reproducing the asymptotic behaviour as observed in Fig. 2. Regarding the density dependence of the coefficients, a simple quadratic proved to be sufficient,

$$\begin{aligned} A_0(\rho_s^*) &= \alpha_{00} + \alpha_{01}\rho_s^* + \alpha_{02}\rho_s^{*2}, \\ A_1(\rho_s^*) &= \alpha_{10} + \alpha_{11}\rho_s^* + \alpha_{22}\rho_s^{*2}, \\ &\cdots \\ B_0(\rho_s^*) &= \beta_{00} + \beta_{01}\rho_s^* + \beta_{02}\rho_s^{*2}, \\ &\cdots \\ C_2(\rho_s^*) &= \gamma_{20} + \gamma_{21}\rho_s^* + \gamma_{22}\rho_s^{*2}. \end{aligned} \quad (36)$$

The model constant α_{i0}, β_{i0}, and γ_{i0} with $i = \{0\ 1\ 2\}$ govern the low-density limit; accordingly, these were correlated to the data for $d(T^*, m, \rho_s^* = 0)$ as obtained from Eq. (31). As can be observed in Fig. 2, the correlation is excellent. To obtain the remaining model constants, we assumed the LHrc EoS for the reference fluid and correlated our MC simulation results for the isothermal pressure of soft-chain fluids of length $m = \{1\ 2\ 3\ 4\}$ at various temperatures T^* (see supplementary material for MC data[62]). A very good regression result is obtained, with an average percentage relative deviation per datapoint of 0.32% (compared to a deviation of 4.06% if no ρ_s^*-dependence is included). To validate the use of Eq. (32) for chain lengths larger than included in the parameter regression, we calculated the isothermal pressure and chemical potential of soft 8-mer fluids for various T^* from GCMC simulations. In Fig. 3, we compare simulations to theory. Excellent agreement is obtained, suggesting the chain-length dependence is well

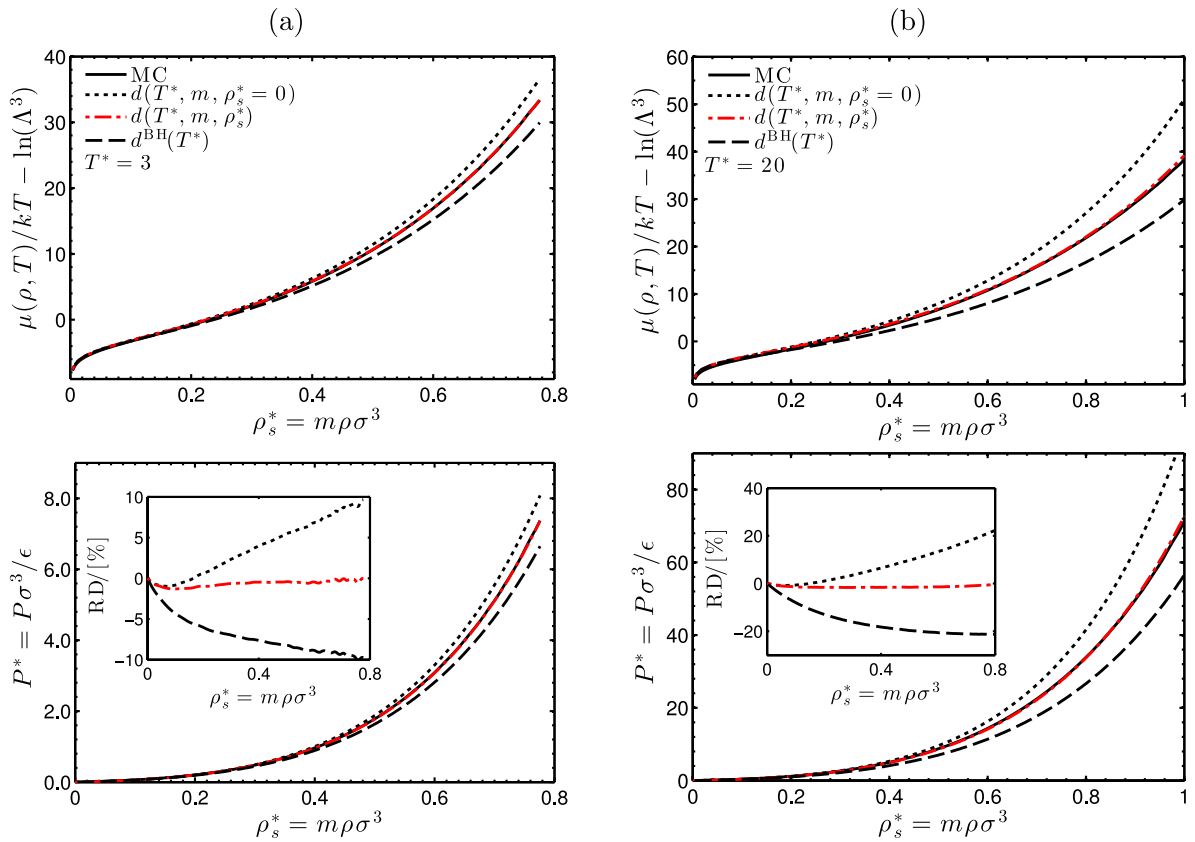

FIG. 3. Isothermal pressure and density-dependent part of the chemical potential of a soft BH repulsive 8-mer at (a) $T^* = 3$ and (b) $T^* = 20$, as obtained from MC simulations and theory. Theoretical results are obtained from the LHrc EoS, using the newly developed effective segment size from Eq. (32) (red, dashed-dotted lines), its low density limit (dotted lines), and the Barker-Henderson diameter (dashed lines), respectively. The figure in the inset shows the percentage relative deviation (RD) of the theoretical results to simulation data. Simulation data are provided in the supplementary material of this work.[62]

TABLE I. The model constants needed to calculate the effective segment size from Eqs. (32)–(36).

i	0	1	2
α_{0i}	0.307 98	0.005 138 8	0.011 117
α_{1i}	0.012 390	0.011 109	−0.039 209
α_{2i}	−0.089 339	−0.030 677	0.016 732
β_{0i}	0.342 22	0.033 920	−0.016 202
β_{1i}	−0.002 499 3	−0.044 614	0.022 757
β_{2i}	−0.093 741	0.017 545	−0.033 500
γ_{0i}	0.000 963 76	0.000 372 70	0.000 083 571
γ_{1i}	−0.000 432 61	−0.000 449 12	−0.000 314 74
γ_{2i}	−0.000 331 33	−0.000 041 420	0.000 446 15

correlated. The model constants needed to calculate $d(T^*, m, \rho_s^*)$ from Eq. (32) are listed in Table I.

It is important to note that the use of the LHrc EoS in obtaining part of the model constants of Eq. (36) does not limit the application of Eqs. (32)–(36) to this hard-chain reference EoS only. For the chain lengths ($m = \{1\ 2\ 3\ 4\}$) and densities involved in the fitting, the LHrc EoS is as accurate as molecular simulations results; therefore, the effective segment size calculated from Eq. (32) can be considered general and can be used in combination with any hard-chain reference EoS.

To quantify the effect of chain flexibility on the effective segment size, we used the second virial method from Eq. (31) to calculate the low-density limit $d(T^*, m, \rho_s^* = 0)$ for linear ($\chi_R = 1.0$), partially flexible ($\chi_R = 0.5$), and semi-flexible (with harmonic bond-bending potential $u_b = \epsilon_b[\theta - \pi]^2$ and $\epsilon_b = 10$) chains of length 8. In Fig. 4, we compare the results to those previously calculated for fully flexible ($\chi_R = 0$) 8-mers. The differences are small. While, in principle, the correlation for $d(T^*, m, \rho_s^*)$ from Eq. (32) is strictly developed for fully flexible chain fluids, these results suggest it could also provide a reasonable approximation for the effective segment size of chains of different flexibility constraints.

In summary, we propose an accurate EoS for BH-repulsive chain fluids (Eqs. (10)–(18) and (32)) that serves as a reference for the development an EoS for LJ chains with variable degree of molecular flexibility.

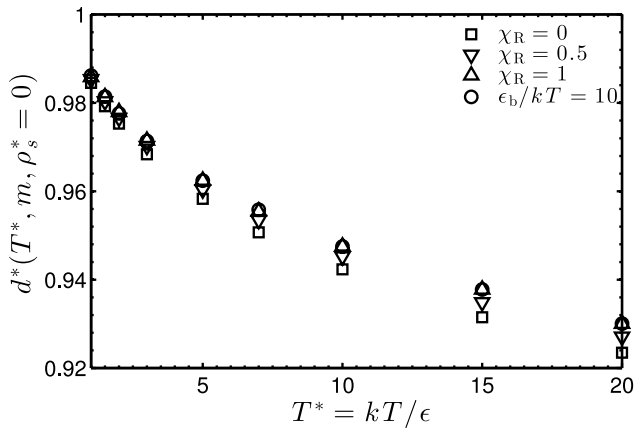

FIG. 4. The effect of intramolecular flexibility on the low-density limit of the reduced effective segment diameter $d^*(T^*, m, \rho_s^* = 0) = d(T^*, m, \rho_s^* = 0)/\sigma$. Results are shown for linear ($\chi_R = 1$), partially flexible ($\chi_R = 0.5$), fully flexible ($\chi_R = 0$), and semi-flexible ($U_b = \epsilon_b[\theta - \pi]^2$, $\epsilon_b = 10$) chain fluids of length 8. The results are obtained from equating second virial coefficients of hard- and soft-chain fluids (see Sec. IV C for details).

D. Simplified perturbation terms

It is now our target to obtain simple analytical functions for the correlation integrals from Eqs. (27)–(30). Since the description of SW chain fluids does not involve the use of any effective segment size, the correlation integrals of SW-chains depend solely on chain length m and packing fraction η. For LJ chain fluids, an additional temperature dependence exists.

Using tabulated MC data for the average segment-segment rdf of the hard-chain reference system, taken from Refs. 44 ($m = 1$), 43 ($m = \{2\ 8\}$), and 41 ($m = \{3\ 4\ 5\ 6\ 7\ 8\}$), respectively, we calculated the correlation integrals over a range in packing fraction $\eta = \{0\text{-}0.5\}$ (the exact range depending on the MC data for rdf) and dimensionless temperature $T^* = \{0.6\ 0.8\ 1.0\ 1.2\ 1.4\ 1.6\ 1.8\ 2.0\ 2.2\ 2.4\ 2.8\ 3.4\ 3.8\ 4.2\ 5\ 6\ 8\ 10\ 15\ 20\}$ (only for LJ). In the calculations for LJ chain fluids, the effective segment size was obtained from Eq. (32). Moreover, for LJ chain fluids, we included additional data for I_2 of a chain molecule of $m = 100\,000$ at a packing fraction $\eta = 10^{-7}$ in the fitting. The values of I_2 for this case were set to 40% of the PY2 result. The reason for doing this is to avoid unphysical negative values of I_2 for very long ($m > 100$) chain fluids. For both SW and LJ chain fluids, the results were correlated by the following power law in packing fraction:

$$I_1^{SW}(m,\eta) = \sum_{i=0}^{4} a_i^{SW}(m)\eta^i, \tag{37}$$

$$I_2^{SW}(m,\eta) = \sum_{i=0}^{4} b_i^{SW}(m)\eta^i, \tag{38}$$

$$I_1^{LJ}(m,\eta,T^*) = \sum_{i=0}^{4} a_i^{LJ}(m,T^*)\eta^i, \tag{39}$$

$$I_2^{LJ}(m,\eta,T^*) = \sum_{i=0}^{4} b_i^{LJ}(m,T^*)\eta^i, \tag{40}$$

where the chain-length dependence of the coefficients a_i and b_i is again obtained from the functional form of Hu, Liu, and Prausnitz,[10,38]

$$a_i^{SW}(m) = a_{i0}^{SW} + a_{i1}^{SW}\frac{m-1}{m} + a_{i2}^{SW}\frac{m-1}{m}\frac{m-2}{m}, \tag{41}$$

$$b_i^{SW}(m) = b_{i0}^{SW} + b_{i1}^{SW}\frac{m-1}{m} + b_{i2}^{SW}\frac{m-1}{m}\frac{m-2}{m}, \tag{42}$$

$$a_i^{LJ}(m,T^*) = a_{i0}^{LJ}(T^*) + a_{i1}^{LJ}(T^*)\frac{m-1}{m} + a_{i2}^{LJ}(T^*)\frac{m-1}{m}\frac{m-2}{m}, \tag{43}$$

$$b_i^{LJ}(m,T^*) = b_{i0}^{LJ}(T^*) + b_{i1}^{LJ}(T^*)\frac{m-1}{m} + b_{i2}^{LJ}(T^*)\frac{m-1}{m}\frac{m-2}{m}. \tag{44}$$

For SW chains, a total of 15 adjustable model constants were used for the fitting (see Table II). For LJ chain fluids, the additional temperature dependence resulted in a total of 31 adjustable model constants. Both the temperature dependence

TABLE II. Model constants needed to calculate the coefficients a_i^{SW} (Eq. (41)) for calculating the first correlation integral $I_1^{SW}(\eta, m)$ (Eq. (37)) of SW chain fluids. The coefficients b_i^{SW} (Eq. (42)) needed to calculate the second correlation integral $I_2^{SW}(\eta, m)$ (Eq. (38)) are obtained from the exact relation $b_i^{SW} = (i+1)a_i^{SW}$.

i	a_{i0}^{SW}	a_{i1}^{SW}	a_{i2}^{SW}
0	0.790 49	−0.595 12	−0.158 24
1	1.123 2	0.491 31	−0.103 93
2	0.076 584	0.887 50	0.537 47
3	−1.401 9	−0.035 067	−0.020 518
4	−1.908 0	−0.725 97	−0.512 81

and the model constants are displayed in Table III. The regression result is excellent, with an average relative deviation per data point of 0.3% for I_1^{LJ} and 0.5% for I_2^{LJ}. For SW chain fluids, the results are of similar accuracy. A graphical representation of the correlation results is presented in Fig. S1 of the supplementary material.[62]

V. RESULTS AND DISCUSSION

In this section, we proceed by comparing theoretical predictions for VLE and isotherms of both, pure fluids, and mixtures to results obtained from molecular simulations. Additionally, the effect of molecular flexibility on the phase behavior is investigated. An extension of the perturbation theory to mixtures is included in the supplementary material of this work.[62]

A. Fully flexible SW chains

We start our analysis for SW chain fluids. SW fluids represent the most basic test of perturbation theory, because the reference fluid is temperature independent.

In Fig. 5, we compare the VLE of several fully flexible SW chain fluids as obtained from the perturbation theory to results obtained from molecular simulations.[12,15,69] For the regarded chain lengths, very good agreement between theory and simulations is observed. For comparison, we included theoretical results as obtained from the SAFT-VR EoS of Gil-Villegas *et al.*[16] As for the EoS developed in this work, the SAFT-VR EoS is based on a second order BH perturbation theory with the LCA for the second order perturbation contribution. The difference is that the SAFT-VR approach is based on a spherical reference fluid (perturbed-sphere method).

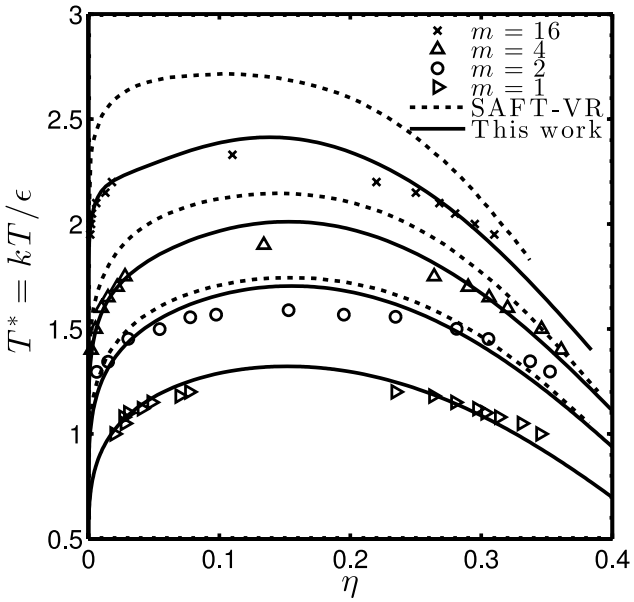

FIG. 5. VLE of fully flexible SW chain fluids. The solid lines are results from the perturbation theory developed in this work. The dotted lines are calculations based on the SAFT-VR EoS of Gil-Villegas *et al.*[16] The symbols are MC simulation results of Vega *et al.*[69] ($m = 1$), Yethiraj and Hall[88] ($m = 2$), and Escobedo and de Pablo[15] ($m = 4$, $m = 16$).

In Fig. 6, we proceed by comparing isotherms of SW chain fluids as obtained from the perturbation theory to molecular simulation results.[14,15] For all temperatures included, good agreement is obtained. For comparison, we included some results obtained from using the TPT1 EoS[3,5] for the hard-chain reference fluid. As can be observed, the use of this EoS leads to a weaker description of simulation data.

In Figs. 7 and 8, we analyze the performance of the EoS in describing molecular simulation results[70,71] for VLE and isotherms of SW-chain fluid mixtures. The VLE are presented in terms of reduced variables (i.e., relative to critical properties). A representation in reduced variables eliminates any inaccuracies introduced by the small overestimation of the pure-component critical properties (see Fig. 5). Agreement between

TABLE III. Temperature dependence and model constants needed to calculate the coefficients $a_i^{LJ\,a}$ (Eq. (43)) and $b_i^{LJ\,b}$ (Eq. (44)) for calculating the first correlation integral $I_1^{LJ}(\eta, m, T^*)$ (Eq. (39)) and second correlation integral $I_2^{LJ}(\eta, m, T^*)$ (Eq. (40)) of LJ chain fluids, respectively.

i	a_{i0}^{LJ}/b_{i0}^{LJ}	a_{i1}^{LJ}/b_{i1}^{LJ}	a_{i2}^{LJ}/b_{i2}^{LJ}
0	$p(1)$	$p(11)$	$p(22)$
1	$p(2)+p(3)\sqrt{T^*}$	$p(12)+p(13)\sqrt{T^*}$	$p(23)$
2	$p(4)+p(5)\sqrt{T^*}$	$p(14)+p(15)\sqrt{T^*}$	$p(24)+p(25)\sqrt{T^*}+p(26)T^*$
3	$p(6)+p(7)\sqrt{T^*}+p(8)T^*$	$p(16)+p(17)\sqrt{T^*}+p(18)T^*$	$p(27)+p(28)\sqrt{T^*}+p(29)T^*$
4	$p(9)+p(10)\sqrt{T^*}$	$p(19)+p(20)\sqrt{T^*}+p(21)T^*$	$p(30)+p(31)\sqrt{T^*}$

[a] $\boldsymbol{p}$ = [−0.8891, −0.7272, 0.026 75, −0.6859, 0.8927, 3.432, −1.364, −0.1390, −1.702, 1.269, 0.4016, −0.3407, −0.2923, −0.6860, −0.3161, −3.007, 3.256, 0.011 25, 6.271, −3.800, 0.1086, 0.4057, −2.145, 9.963, 0.5556, 0.099 79, −20.30, −3.779, −0.1887, 13.53, 5.007].

[b] $\boldsymbol{p}$ = [0.4065, 0.6205, −0.022 78, −0.029 08, −0.4997, 1.008, −0.032 63, 0.1068, −3.432, 0.2455, −0.2902, 0.1989, 0.1308, −0.1802, 0.4156, 2.426, −0.6577, −0.1061, −1.999, −0.9246, 0.1546, −0.096 34, −0.1705, 0.6318, −0.2604, −0.022 58, −0.4699, 0.9034, 0.015 21, −0.2431, −0.1696].

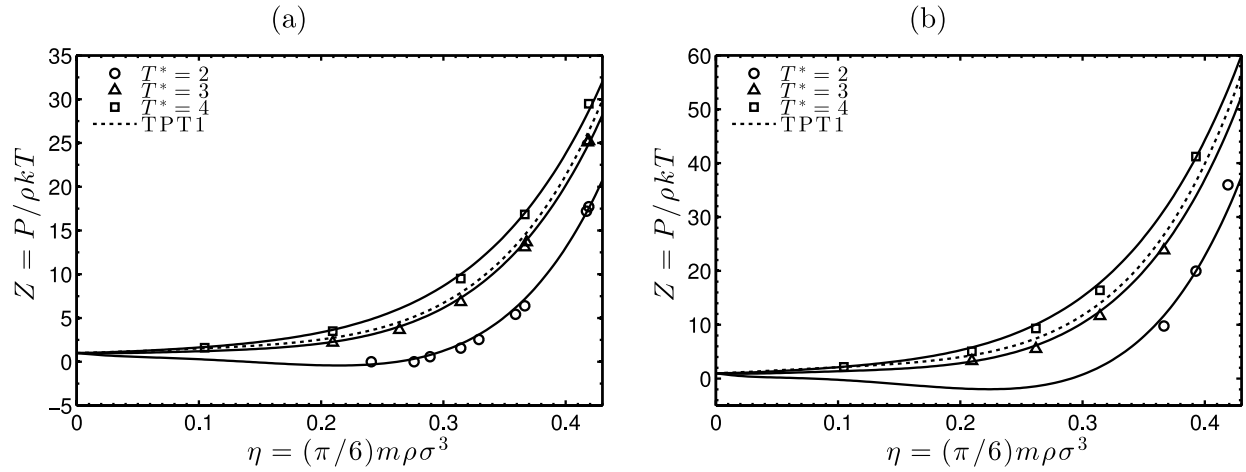

FIG. 6. Isotherms of (a) a fully flexible SW 8-mer and (b) a fully flexible SW 16-mer. Lines are results obtained from the perturbation theory developed in this work using the LHrc EoS (solid lines) and the TPT1 EoS (for $T^* = 3$, dotted lines) to describe the hard-chain reference fluid. Symbols are MC data of Escobedo and de Pablo[15] ($m = 8$) and Tavares *et al.*[14] ($m = 8$, $m = 16$).

simulations and theory is satisfactory and is comparable to that obtained from the SAFT-VR EoS.[70]

B. Fully flexible LJ chains

In Fig. 9, the VLE of fully flexible LJ chain fluids as obtained from the perturbation theory developed in this work is compared to the results from MC simulations.[15,72–76] For both the vapor-liquid coexistence densities and vapour pressure, we find satisfactory agreement between theory and simulations. Especially, the description of vapor pressures is noteworthy.

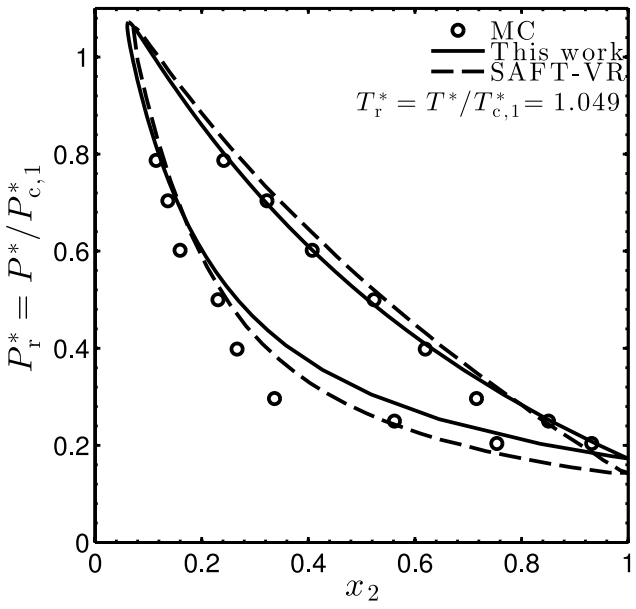

FIG. 7. Dimensionless pressure ($P^* = P\sigma_{11}^3/\epsilon_{11}$) vs. mole fraction ($x_2$) representation of the VLE of a binary mixture of SW monomers (component 1) and SW dimers (component 2) at a reduced temperature of $T_r^* = T^*/T_{c,1}^* = 1.049$, where $T^* = kT/\epsilon_{11}$ and $T_{c,1}$ is the critical temperature of the pure monomeric fluid. Solid lines are results obtained from the perturbation theory developed in this work ($T_{c,1}^* = 1.3219$, $P_{c,1}^* = 0.142\,70$). Dashed lines are calculations based on the SAFT-VR EoS.[70] Symbols are MC data of Davies *et al.*[70] ($T_{c,1}^* = 1.22$, $P_{c,1}^* = 0.108$).

We should stress that, compared to Fig. 1, the improved results shown here are a result of the effective segment size from Eq. (32). The overall satisfactory agreement between theory and simulation, however, is a result of all three ingredients of the perturbation theory, namely, the accurate EoS for the reference fluid, the effective segment size from Eq. (32), and the MC data for the averaged segment-segment rdf of the hard-chain reference fluid. To demonstrate the effect of using a reference EoS different than the LHrc EoS, we included results for the VLE of a LJ 50-mer based on the TPT1 EoS[3] and TPT2 EoS[4] for the hard-chain reference fluid. Especially in the intermediate density region, TPT loses some of its accuracy for chains longer than 8 segments. As shown in Fig. 9, these inaccuracies result in a rather poor description of the VLE of LJ 50-mers.

As could be expected from a perturbation theory up to second order, the critical temperature is overestimated for all systems considered. For chain lengths $m = 1$ and $m = 2$, we find a small underestimation of coexistence densities in the dense liquid phase. As pointed out by Paricaud,[64] discrepancies

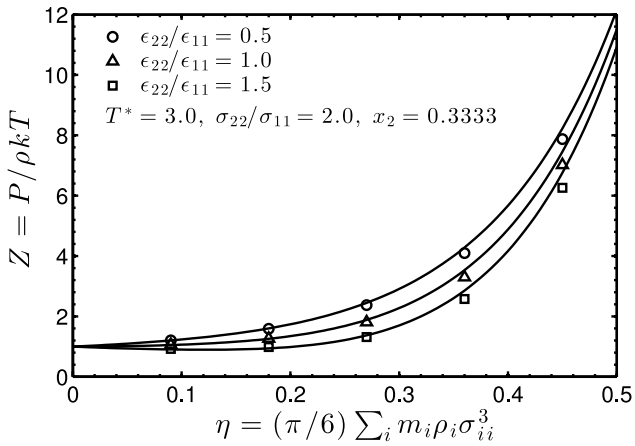

FIG. 8. Compressibility factor $Z = P/\rho kT$ of several asymmetric binary mixtures of SW monomers (component 1) and SW dimers (component 2) at a dimensionless temperature of $T^* = kT/\epsilon_{11} = 3.0$. Solid lines are results obtained from the perturbation theory developed in this work. Symbols are MD data of Gulati and Hall.[71]

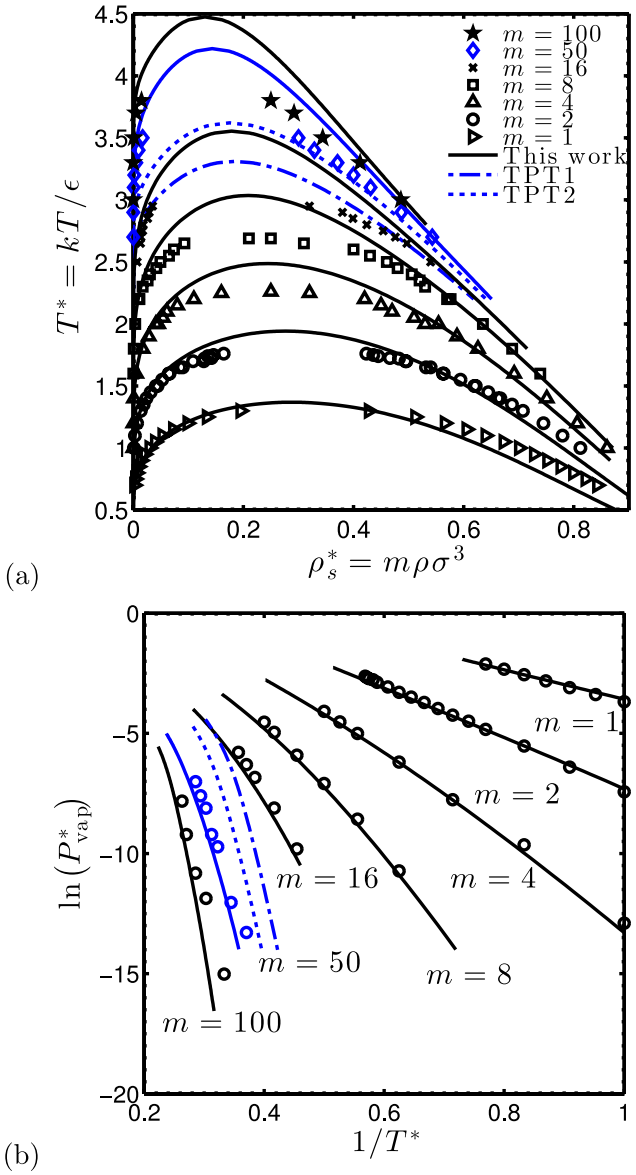

FIG. 9. The VLE of fully flexible LJ chain fluids of segment number m. Diagram (a) shows the coexistence densities and (b) presents the saturated vapour pressure $P^*_{vap} = P_{vap}\sigma^3/\epsilon$. The solid lines are results from the perturbation theory developed in this work, based on the LHrc EoS for the reference fluid. For comparison, we included some results based on the TPT1 EoS (dashed-dotted lines) and TPT2 EoS (dotted lines) for the reference fluid. Symbols are MC simulation results of Lotfi *et al.*[72] ($m = 1$), Vega *et al.*[73] ($m = 2$), Dubey *et al.*[74] ($m = 2$), MacDowell and Blas[76] ($m = 4$, $m = 8$, $m = 16$), Escobedo and de Pablo[15] ($m = 4$, $m = 8$, $m = 16$), and Sheng and Panagiotopoulos[75] ($m = 50$, $m = 100$).

of this kind are caused by the use of the LCA for the second order perturbation term. The reason these underestimations are not observed for larger chain lengths could be due to the larger overestimation of the critical temperature of these fluids, which leads to a shift of liquid coexistence densities to somewhat larger values. Another reason could be small inaccuracies in the correlation integrals I_1^{LJ} and I_2^{LJ} (Eqs. (39) and (40)) for chain lengths longer than those used in their development. We observed that, compared to the first correlation integral, the second correlation integral converges more slowly to its asymptotic value at large chain lengths. Therefore, it might be that in the development of I_2^{LJ} (Eq. (40)), we did not include sufficient MC data for the hard-chain rdf of long chain fluids. Although there are MC data for the rdf of longer ($m = 20$, $m = 50$, $m = 100$) hard-sphere chain fluids available in the literature,[77] we found that inclusion of these data in the calculation of the correlation integrals leads to irregular scaling behaviour with chain length m. For this reason, we choose not to include additional MC data for the rdf of longer hard-chain fluids in the calculation of the correlation integrals.

It is instructive to compare the results obtained from our perturbed-chain method to those obtained from a perturbation theory based on a spherical reference fluid (perturbed-sphere method). Perturbed-sphere equations of state that were developed on equal grounds as the perturbed-chain EoS presented in this work (i.e., 2nd order Barker Henderson theory, LCA for a_2, no correlation to simulation data of attractive chain fluids) are the SAFT-VR LJ EoS of Davies *et al.*[63] and the 2006 version of the SAFT-VR Mie EoS of Lafitte *et al.*[28] It is noteworthy that other perturbed-sphere methods are available that perform better than SAFT-VR LJ and SAFT-VR Mie 2006. State-of-the-art models, in this respect, are the soft-SAFT EoS of Blas and Vega[26] (which was developed based on the EoS of Johnson and Gubbins[22,78]) and the 2013 version of the SAFT-VR-Mie EoS of Lafitte *et al.*[27] For soft-SAFT, the description of the LJ-sphere reference fluid is obtained from an accurate empirical EoS.[78] The SAFT-VR Mie approach describes the LJ-sphere reference fluid based on a third order BH perturbation theory. The second and third order perturbation terms of this approach were parametrized to macroscopic properties, namely, to MC results for the VLE of Mie chain fluids. In Fig. 10, we compare VLE and vapor pressures as obtained from the SAFT-VR LJ EoS, SAFT-VR Mie 2006 EoS, and SAFT-VR Mie 2013 EoS to those obtained from the EoS developed in this work. As expected, the SAFT-VR Mie 2013 EoS results in the most accurate description of saturated liquid densities and the critical region. For vapor phase properties, however, the perturbation theory developed in this work results in the most faithful description of simulation data.

In Fig. 11, we compare isothermal pressures as obtained from the perturbation theory to results from MC simulations.[22,78] For all temperatures and chain lengths considered, agreement between theory and simulations is excellent. As can be observed in Fig. 11(b), the use of a density-dependent segment size $d(T^*, m, \rho_s^*)$ is essential to come to a reliable description of simulation data. When the original BH diameter $d^{BH}(T^*)$, or the low-density limit $d(T^*, m, \rho_s^* = 0)$, is used instead, isothermal pressures are under- and overestimated, respectively.

In Figs. 12 and 13, theoretical predictions for VLE and isothermal pressures of LJ chain-fluid mixtures are compared to results obtained from molecular simulations.[26,79] Given that the mixtures involve triple (m, σ, and ϵ) asymmetries, agreement between simulations and theory is very satisfactory.

C. Effect of molecular flexibility on VLE

We now turn to the effect of molecular flexibility on the VLE. In order to study this, we performed GCMC simulations to calculate the VLE of fully flexible and rigid linear SW- ($m = 4$) and LJ chain fluids ($m = \{3\ 4\ 5\}$). Also, we calculated

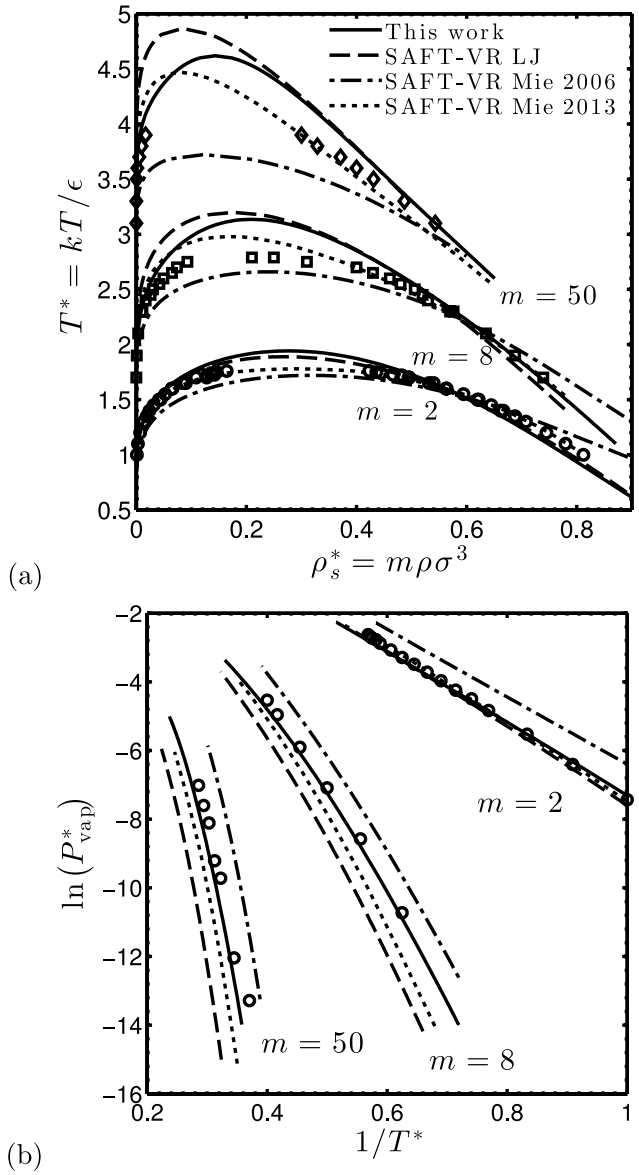

FIG. 10. The VLE of fully flexible LJ chain fluids of segment number m, as obtained from the perturbation theory developed in this work (solid lines), the SAFT-VR LJ EoS[63] (dashed lines), the SAFT-VR Mie 2006 EoS[28] (dashed-dotted lines), the SAFT-VR Mie 2013 EoS[27] (dotted lines), and MC simulations (symbols). Diagram (a) shows the coexistence densities and (b) presents the saturated vapour pressure $P_{\rm vap}^* = P_{\rm vap}\sigma^3/\epsilon$. For visual clarity, the coexistence temperature T^* in (a) is shifted upwards by 0.1 for $m = 8$ and by 0.4 for $m = 50$. MC simulation results included are those of Vega *et al.*[73] ($m = 2$), Dubey *et al.*[74] ($m = 2$), MacDowell and Blas[76] ($m = 8$), Escobedo and de Pablo[15] ($m = 8$), and Sheng and Panagiotopoulos[75] ($m = 50$).

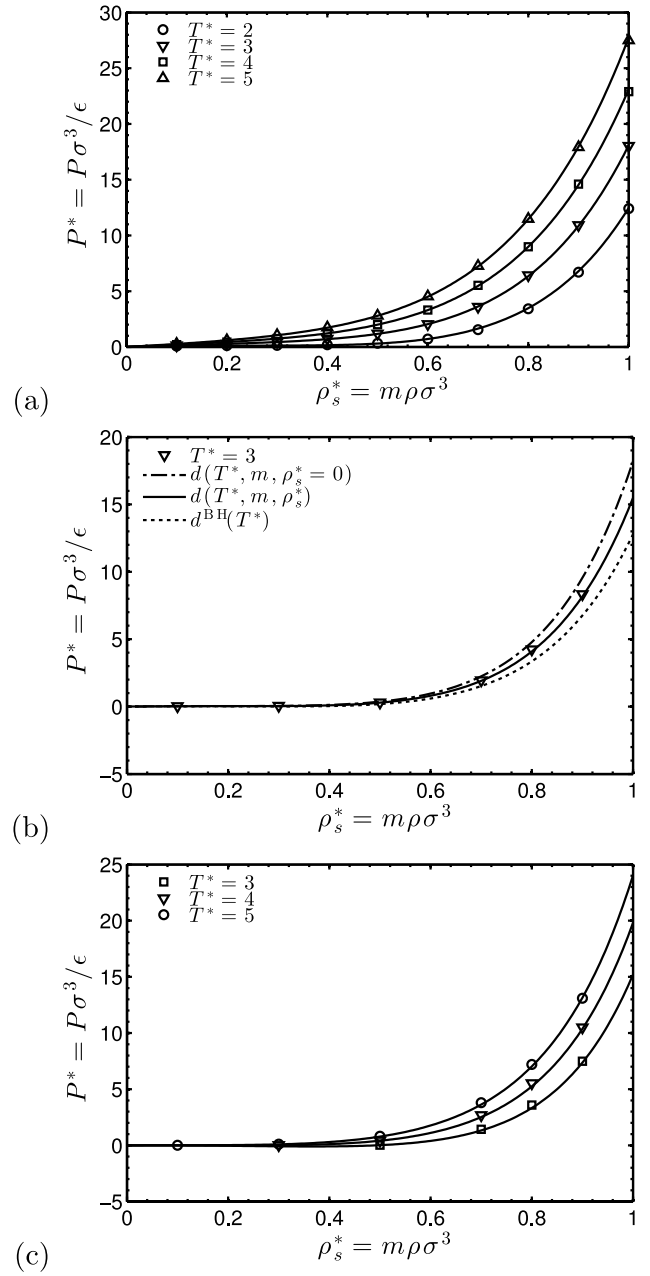

FIG. 11. Isothermal pressure of fully flexible LJ chain fluids of (a) $m = 2$, (b) $m = 8$, and (c) $m = 100$. Theoretical results are obtained from the perturbation theory developed in this work, using the newly developed effective segment size from Eq. (32) (solid lines), its low density limit (dashed-dotted lines), and the Barker-Henderson diameter (dotted lines), respectively.

the VLE of partially flexible 4-3 SW rod-coils. For simulation data, the reader is referred to the supplementary material of this work.[62] In Fig. 14, we compare simulation results to those from the literature, as obtained by Escobedo and de Pablo[15] (fully flexible SW 4-mers), Galindo *et al.*[34] (rigid linear LJ 5-mers), MacDowell and Blas[76] (fully flexible LJ 4-mers), and Blas *et al.*[80,81] (fully flexible- and rigid linear LJ 3-, 4-, and 5-mers). Please note that to allow for a clear distinction of simulation results, the results for LJ 4- and 5-mers are shifted upwards (in T^*) by 0.2 and 0.4, respectively. Good agreement between different simulation results is obtained. Upon increasing the rigidity of the chains, our simulations show (1) a widening of the VLE (i.e., smaller saturated vapor density and larger saturated liquid density), (2) an increase of the critical temperature T_c, and (3) a decrease of the critical density ρ_c.

In Fig. 15, we compare simulation results for fully flexible-, partially flexible-, and rigid linear SW 4-mers to those obtained from the perturbation theory developed in this work. Please note that for other chain lengths than those shown in Fig. 15, the theory predicts the same trends with molecular rigidity. Both simulations and theory predict an increase of the VL critical temperature with increasing rigidity of the chains. Moreover, the widening of the VL region for chains of increased rigidity is at least qualitatively captured. The effect

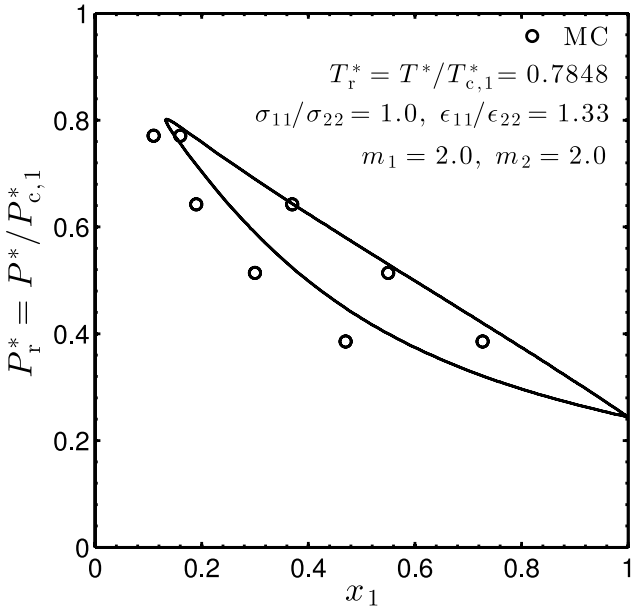

FIG. 12. Dimensionless pressure ($P^* = P\sigma_{11}^3/\epsilon_{11}$) vs. mole fraction ($x_1$) representation of the VLE of an asymmetric binary mixture of LJ dimers ($\sigma_{11}/\sigma_{22} = 1.0$, $\epsilon_{11}/\epsilon_{22} = 1.33$) at a reduced temperature of $T_r^* = T^*/T_{c,1}^* = 0.7848$, where $T^* = kT/\epsilon_{11}$ and $T_{c,1}$ is the critical temperature of a pure fluid of component 1. Solid lines are results obtained from the perturbation theory developed in this work ($T_{c,1}^* = 1.9421$, $P_{c,1}^* = 0.104\,39$). Symbols are MC data of Blas and Vega.[26] For simulation results, the critical properties of the pure fluid of component 1 were obtained from the MC data of Vega *et al.*[73] using conventional scaling laws ($T_{c,1}^* = 1.784$, $P_{c,1}^* = 0.077\,84$). Please note that our critical pressure is different than that obtained in the original paper of Vega *et al.*[73] due to an error in their application of the Clausius-Clapeyron equation.

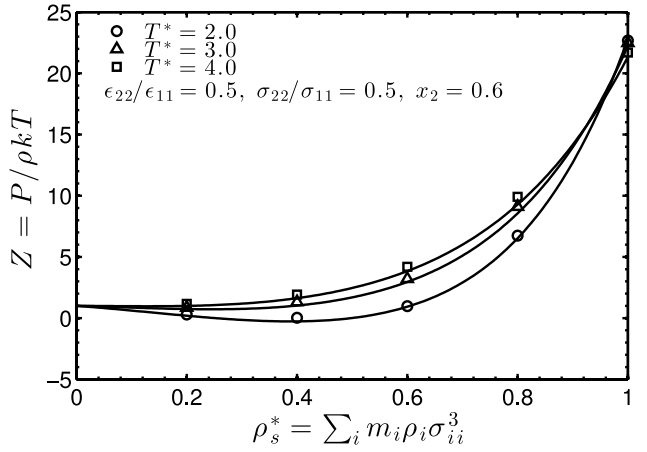

FIG. 13. Compressibility factor $Z = P/\rho kT$ vs. dimensionless segment density ρ_s^* of an asymmetric binary mixture of LJ 4-mers (component 1) and LJ 8-mers (component 2) at several dimensionless temperatures $T^* = kT/\epsilon_{11}$. Solid lines are results obtained from the perturbation theory developed in this work. Symbols are MD data of Reis *et al.*[79]

of molecular rigidity on the liquid side of the diagram is more accurately predicted than the effect on the vapor side. For the vapor side, agreement with simulations is only qualitative. The reason for this is most probably that our use of a rdf of fully flexible hard-sphere chains in the calculation of the perturbation terms of rigid linear- and partially flexible chains is more harsh an approximation at low densities. Altogether, given that the theory only includes the effect of molecular flexibility through the reference fluid, we view the agreement between theory and simulations as very promising.

As we show in Fig. 16, the effect of flexibility on the VLE of LJ chain fluids is less well described than for SW chain fluids. As for SW chains, the perturbation theory gives the wrong trend of the critical density with flexibility. For LJ chains, however, the trends of the critical temperature and vapor density with flexibility of the chains are also incorrectly predicted. The theory does capture the effect of molecular flexibility on the liquid densities. The weaker results for the effect of flexibility on the VLE of LJ chain fluids (compared to SW chains) are caused by the use of the effective segment size. One might suspect that a lacking of any χ_R-dependence in $d(T^*, m, \rho_s^*)$ could be the underlying reason. However, the results from Fig. 4 suggest the effective segment size of rigid

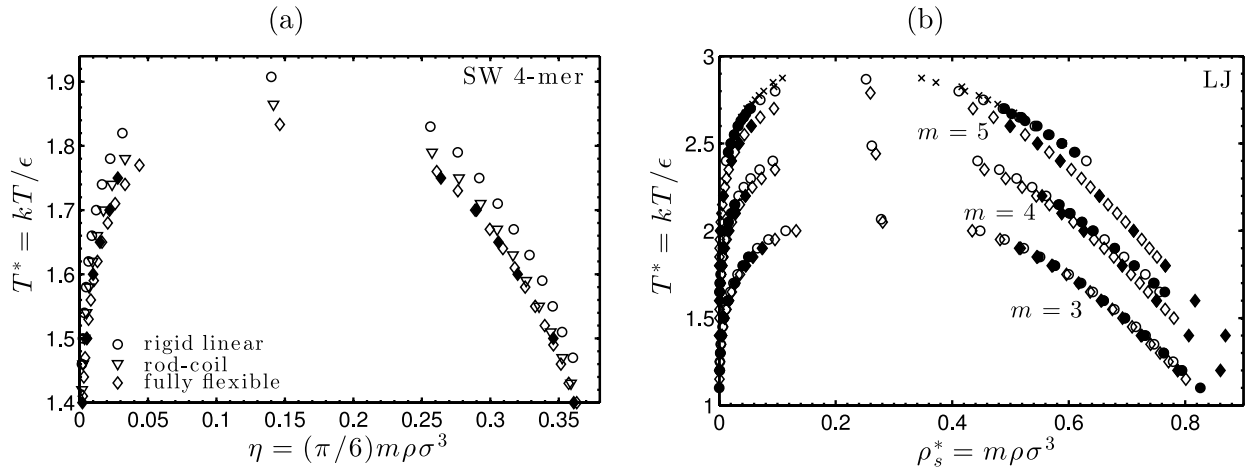

FIG. 14. The VLE of fully flexible (diamonds), rod-coil partially flexible (triangles), and rigid linear (circles, crosses) SW- and LJ chain fluids as obtained from MC simulations performed in this work (open symbols) and the literature (closed symbols, crosses). For visual clarity, the results for LJ chains of $m = 4$ and $m = 5$ are shifted upwards by 0.2 and 0.4, respectively. The literature data included in this figure are those of Escobedo and de Pablo[15] (fully flexible SW 4-mers), MacDowell and Blas[76] (fully flexible LJ 4-mers), Blas *et al.*[80,81] (fully flexible LJ 3- and 5-mers, rigid linear LJ 3-, 4- and 5-mers) and Galindo *et al.*[34] (rigid linear LJ 5-mers). The data of Galindo *et al.*[34] are shown by the crosses. For results of the simulations performed in this work, the reader is referred to the supplementary material.[62]

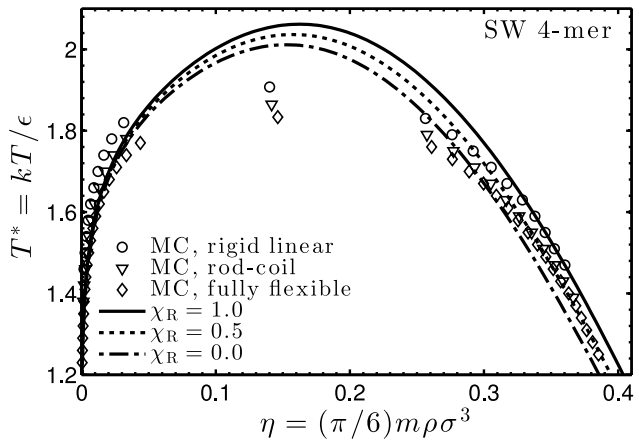

FIG. 15. The VLE of fully flexible- (diamonds, dashed-dotted line), rod-coil partially flexible (triangles, dotted line), and rigid linear (circles, solid line) SW 4-mers as obtained from the perturbation theory developed in this work (lines) and molecular simulations of this work (symbols).

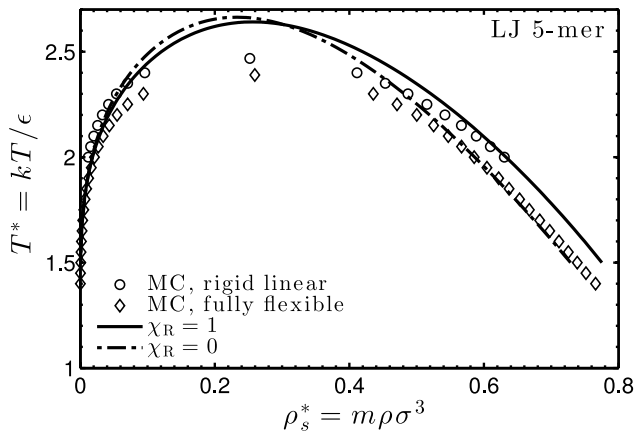

FIG. 16. The VLE of fully flexible- (diamonds, dashed-dotted line) and rigid linear (circles, solid line) LJ 5-mers as obtained from the perturbation theory developed in this work (lines) and molecular simulations of this work (symbols).

linear chain fluids is somewhat larger than that of fully flexible chains, corresponding to a lower (not higher) critical temperature. A more probable cause of errors is the use of a hard-chain rdf of segment size d and bond-length d in the calculation of the correlation integrals, Eqs. (29) and (30). Considering a hard-chain fluid with segment diameter d and bond-length d is not strictly correct, because the segment distance should be σ. In future work, we plan to evaluate the effect of this approximation by comparing our perturbation terms to those obtained from MC simulations.

VI. CONCLUSION

We have developed two new perturbed-chain equations of state for attractive chain fluids with varying degree of flexibility. The two models are for tangent SW- and LJ chain fluids and their mixtures in isotropic (vapor and liquid) phases. The EoS was derived in the framework of a 2nd order Barker-Henderson perturbation theory. To arrive at a satisfactory comparison of calculated VLE of flexible SW- and LJ chain fluids to those obtained from molecular simulations, some modifications to the original recipe of Barker and Henderson were required. First, it was shown that the original BH diameter is insufficient for approximating the soft repulsion between the segments of LJ chain fluids. A new effective segment size was developed that explicitly incorporates the chain-connectivity of segments. The new segment size was shown to be density dependent. Second, it was demonstrated that small inaccuracies in the rdf of the hard-chain reference fluid can lead to significant errors in calculated VLE. We showed that these errors are small if a rdf obtained directly from MC simulations is used. Finally, we showed the importance of using an accurate EoS for the hard-chain reference fluid. In particular, it was shown that commonly used equations of state such as TPT1 lead to poor predictions of VLE of long LJ chains. When using the more accurate LH EoS instead, a much better comparison to MC data was obtained.

Recently, we developed an extension of the LH EoS to partially flexible and rigid linear chain fluids.[11] Using this extended EoS to calculate the reference contribution, it is possible to model the effects of intramolecular flexibility on the VLE of SW- and LJ chain fluids. MC simulations were performed to validate theoretical results. For both SW- and LJ chain fluids, our simulations show the following trends of the VLE with increased rigidity of the chains: (1) a widening of the VLE (larger saturated liquid density and smaller saturated vapor density), (2) a shift of the critical temperature to higher values, and (3) a shift of the critical density to lower values. For SW chain fluids, theoretical results are in good agreement with results from MC simulations; all trends but that of the critical density were correctly predicted. For LJ chain fluids, the theoretical description captured the widening of the vapor liquid envelope with increasing chain rigidity but did not capture the shift of critical properties. We suspect that this is due to our application of an effective segment size in the calculation of the perturbation contributions to the EoS. In future work, we plan to test this by comparing the perturbation terms to those obtained from molecular simulations.

In agreement with previous studies on the subject,[34,80–83] the results of this work show that the effect of molecular flexibility on the isotropic (vapor-liquid) phase behavior of attractive chain fluids is quite small. If the equation of state is coupled to a suitable description of anisotropic phases (such as solids or liquid crystals), however, it is expected these subtle effects can make the difference for an accurate prediction of phase equilibria (see, for example, Ref. 11). An extension of the EoS to anisotropic phases will be developed in future work.

ACKNOWLEDGMENTS

This research is supported by the Stichting voor Technische Wetenschappen (Dutch Technology Foundation, STW), applied science division of the Nederlandse organisatie voor Wetenschappelijk Onderzoek (Netherlands Organization for Scientific Research, NWO), and the Technology Program of the Ministry of Economic Affairs. In addition, this work was sponsored by the Stichting Nationale Computerfaciliteiten (National Computing Facilities Foundation, NCF) for the

use of supercomputing facilities, with financial support from NWO-EW (Grant No. MP-213-14).

APPENDIX: CALCULATING 2ND VIRIAL COEFFICIENTS FROM MC INTEGRATION

For any two chain molecules 1 and 2 interacting via a pair-potential $U(r,\Omega_1,\Omega_2)$, the 2nd virial coefficient is defined as[84]

$$B_2 = -2\pi \int_0^\infty \left(\langle \exp(-\beta U(r,\Omega_1,\Omega_2)) \rangle_{\Omega_1\Omega_2} - 1 \right) r^2 dr. \quad \text{(A1)}$$

Here, r is the separation between the center of mass of molecules 1 and 2, Ω is a vector that describes a molecule's configuration (the orientation vector of the first bond, and all bond- and torsion angles), and $\langle \cdots \rangle_{\Omega_1\Omega_2}$ denotes an ensemble average over all configurations of molecules 1 and 2. Introducing a segment-segment potential $u_{\alpha\beta}$, the energy of the pair interaction U can be calculated from a sum over all segment-segment interactions of the two chain molecules, according to

$$U(r,\Omega_1,\Omega_2) = \sum_\alpha^m \sum_\beta^m u_{\alpha\beta}(r_{\alpha\beta}). \quad \text{(A2)}$$

Introducing a dimensionless separation $x = r_{\alpha\beta}/\sigma$, the segment-segment interactions of hard- and soft-chain fluids are calculated as, respectively,

$$\beta u^{\text{hc}}_{\alpha\beta}(x) = \begin{cases} \infty, & \text{for } x \le 1 \\ 0, & \text{for } x > 1 \end{cases}, \quad \text{(A3)}$$

$$\beta u^{\text{sc}}_{\alpha\beta}(x) = \begin{cases} \dfrac{4}{T^*} x^{-12}, & \text{for } x \le 1 \\ 0, & \text{for } x > 1 \end{cases}. \quad \text{(A4)}$$

To compute the 2nd virial coefficient for a chain fluid of length m, we calculated the ensemble average $\langle \exp(-\beta U_{12}(r,\Omega_1,\Omega_2)) \rangle_{\Omega_1\Omega_2}$ over a grid in $x = [0 \quad 2m]$ (with $\Delta x = 0.01$) and subsequently solved Eq. (A1) by numerical integration. The ensemble average was obtained from 3×10^6 different chain pairs for $m = \{1\ 2\ 3\ 5\}$ and 15×10^6 different chain pairs for $m = \{8\ 16\}$. For each chain pair, the configurations of the two chain molecules were generated independently using the Rosenbluth method.[52,85–87] In this method, a molecule is grown by choosing the orientation of each new bead from a predefined number of trial directions. To remove the bias introduced by this and to retain correct Boltzmann sampling, we used a statistical weight for each chain pair, calculated as the product of the Rosenbluth weights of the individual chain molecules. The standard deviation in the computed 2nd virial coefficient was obtained from five individual calculations. Results of our calculations are included in the supplementary material of this work.[62]

[1] E. A. Müller and K. E. Gubbins, Ind. Eng. Chem. Res. **40**, 2193 (2001).
[2] S. P. Tan, H. Adidharma, and M. Radosz, Ind. Eng. Chem. Res. **47**, 8063 (2008).
[3] M. S. Wertheim, J. Stat. Phys. **42**, 477 (1986).
[4] M. S. Wertheim, J. Chem. Phys. **87**, 7323 (1987).
[5] W. G. Chapman, G. Jackson, and K. E. Gubbins, Mol. Phys. **65**, 1057 (1988).
[6] H. G. Honnell and C. K. Hall, J. Chem. Phys. **90**, 1841 (1989).
[7] Y. Zhou and G. Stell, J. Chem. Phys. **96**, 1507 (1992).
[8] J. Chang and S. I. Sandler, Chem. Eng. Sci. **49**, 2777 (1994).
[9] D. Ghonasgi and W. G. Chapman, J. Chem. Phys. **100**, 6633 (1994).
[10] Y. Hu, H. Liu, and J. M. Prausnitz, J. Chem. Phys. **104**, 396 (1996).
[11] T. van Westen, B. Oyarzún, T. J. H. Vlugt, and J. Gross, Mol. Phys. **112**, 919 (2014).
[12] A. Yethiraj and C. K. Hall, J. Chem. Phys. **95**, 8494 (1991).
[13] M. Banaszak, Y. C. Chiew, and M. Radosz, Phys. Rev. E **48**, 3769 (1993).
[14] F. W. Tavares, J. Chang, and S. I. Sandler, Mol. Phys. **86**, 1451 (1995).
[15] F. A. Escobedo and J. J. de Pablo, Mol. Phys. **87**, 347 (1996).
[16] A. Gil-Villegas, A. Galindo, P. J. Whitehead, S. J. Mills, G. Jackson, and A. N. Burgess, J. Chem. Phys. **106**, 4168 (1997).
[17] F. W. Tavares, J. Chang, and S. I. Sandler, Fluid Phase Equilib. **140**, 129 (1997).
[18] J. Gross and G. Sadowski, Fluid Phase Equilib. **168**, 183 (2000).
[19] J. Cui and J. E. Elliott, J. Chem. Phys. **114**, 7283 (2001).
[20] M. Lee, C. McCabe, and P. T. Cummings, Fluid Phase Equilib. **221**, 63 (2004).
[21] W. G. Chapman, K. E. Gubbins, G. Jackson, and M. Radosz, Ind. Eng. Chem. Res. **29**, 1709 (1990).
[22] J. K. Johnson, E. A. Müller, and K. E. Gubbins, J. Phys. Chem. **98**, 6413 (1994).
[23] M. Banaszak, Y. C. Chiew, R. O'Lenick, and M. Radosz, J. Chem. Phys. **100**, 3803 (1994).
[24] D. Ghonasgi and W. G. Chapman, AIChE J. **40**, 878 (1994).
[25] E. A. Müller, L. F. Vega, and K. E. Gubbins, Mol. Phys. **83**, 1209 (1994).
[26] F. J. Blas and L. F. Vega, Mol. Phys. **92**, 135 (1997).
[27] T. Lafitte, A. Apostolakou, C. Avendão, A. Galindo, C. S. Adjiman, E. A. Müller, and G. Jackson, J. Chem. Phys. **139**, 154504 (2013).
[28] T. Lafitte, D. Bessieres, M. M. Piñeiro, and J. Daridon, J. Chem. Phys. **124**, 024509 (2006).
[29] S. Phan, E. Kierlik, and M. L. Rosinberg, J. Chem. Phys. **99**, 5326 (1993).
[30] T. Boublík, C. Vega, and M. Diaz-Penã, J. Chem. Phys. **93**, 730 (1990).
[31] C. McBride and C. Vega, J. Chem. Phys. **117**, 10370 (2002).
[32] D. C. Williamson and G. Jackson, Mol. Phys. **86**, 819 (1995).
[33] T. van Westen, T. J. H. Vlugt, and J. Gross, J. Chem. Phys. **37**, 044906 (2012).
[34] A. Galindo, C. J. Vega, E. Sanz, L. G. MacDowell, and E. de Miguel, J. Chem. Phys. **120**, 3957 (2004).
[35] T. van Westen, B. Oyarzún, T. J. H. Vlugt, and J. Gross, J. Chem. Phys. **139**, 034505 (2013).
[36] J. A. Barker and D. Henderson, J. Chem. Phys. **47**, 2856 (1967).
[37] J. A. Barker and D. Henderson, J. Chem. Phys. **47**, 4714 (1967).
[38] H. Liu and Y. Hu, Fluid Phase Equilib. **122**, 75 (1996).
[39] J. Gross and G. Sadowski, Ind. Eng. Chem. Res. **40**, 1244 (2001).
[40] T. W. Cochran and Y. C. Chiew, J. Chem. Phys. **124**, 224901 (2006).
[41] F. Alavi and F. Feyzi, J. Chem. Phys. **139**, 074104 (2013).
[42] Y. C. Chiew, Mol. Phys. **73**, 359 (1991).
[43] J. Chang and S. I. Sandler, J. Chem. Phys. **102**, 437 (1995).
[44] J. Kolafa, S. Labik, and A. Malijevsky, Presented at 18th IUPAC ICCT, Beijing, China, August 17-21, 2004, MD data can be found at http://www.vscht.cz/fch/software/hsmd/.
[45] H. A. Lorentz, Ann. Phys. **12**, 127 (1881).
[46] D. C. R. Berthelot, Compt. Rend. **126**, 1703 (1898); **126**, 1857 (1898).
[47] P. Virnau and M. Möller, J. Chem. Phys. **120**, 10925 (2004).
[48] V. K. Shen and J. R. Errington, J. Phys. Chem. B **108**, 19595 (2004).
[49] J. R. Errington, J. Chem. Phys. **118**, 9915 (2003).
[50] J. I. Siepmann and D. Frenkel, Mol. Phys. **75**, 59 (1992).
[51] D. Frenkel, G. C. A. M. Mooij, and B. Smit, J. Phys.: Condens. Matter **4**, 3053 (1991).
[52] D. Frenkel and B. Smit, *Understanding Molecular Simulation: From Algorithms to Applications*, 2nd ed. (Academic Press, San Diego, 2002).
[53] N. B. Wilding and M. Müller, J. Chem. Phys. **102**, 2562 (1995).
[54] N. B. Wilding, J. Phys.: Condens. Matter **9**, 585 (1997).
[55] A. Hemmen, J. Gross, and A. Z. Panagiotopoulos, "Grand canonical Monte Carlo simulations guided by an analytic equation of state: Transferable anisotropic Mie potentials for ethers," J. Phys. Chem. B (to be published).
[56] A. Z. Panagiotopoulos, J. Phys.: Condens. Matter **12**, R25 (2000).
[57] J. P. Hansen and I. R. McDonald, *Theory of Simple Liquids*, 3rd ed. (Academic Press, London, 2006).
[58] J. D. Weeks, D. Chandler, and H. C. Andersen, J. Chem. Phys. **54**, 5237 (1971).
[59] K. E. Gubbins, W. R. Smith, M. K. Tham, and E. W. Tiepel, Mol. Phys. **22**, 1089 (1971).
[60] T. Boublík, J. Chem. Phys. **53**, 471 (1970).
[61] G. Mansoori, N. F. Carnahan, K. E. Starling, and T. W. Leland, J. Chem. Phys. **54**, 1523 (1971).

[62]See supplementary material at http://dx.doi.org/10.1063/1.4922264 for I. Results of molecular simulations performed in this work; II. The equations for the simplified reference equation of state, used to calculate LCA related terms; III. An extension of the perturbation theory to mixtures; and IV. Supplemental figures.
[63]L. A. Davies, A. Gil-Villegas, and G. Jackson, Int. J. Thermophys. **19**, 675 (1998).
[64]P. Paricaud, J. Chem. Phys. **124**, 154505 (2006).
[65]Y. Tang, J. Chem. Phys. **116**, 6694 (2002).
[66]D. J. Tildesley and W. B. Street, Mol. Phys. **4**, 85 (1980).
[67]R. Dickman and C. K. Hall, J. Chem. Phys. **89**, 3168 (1988).
[68]R. L. Cotterman, B. J. Schwarz, and J. M. Prausnitz, AIChE J. **32**, 1787 (1986).
[69]L. Vega, E. de Miguel, L. F. Rull, G. Jackson, and M. I. A., J. Chem. Phys. **96**, 2296 (1992).
[70]L. A. Davies, A. Gil-Villegas, G. Jackson, S. Calero, and S. Lago, Phys. Rev. E **57**, 2035 (1998).
[71]H. S. Gulati and C. K. Hall, J. Chem. Phys. **107**, 3930 (1997).
[72]A. Lotfi, J. Vrabec, and J. Fischer, Mol. Phys. **76**, 1319 (1992).
[73]C. Vega, C. McBride, F. J. Blas, and A. Galindo, J. Chem. Phys. **118**, 10696 (2003).
[74]G. S. Dubey, S. O'Shea, and P. A. Monson, Mol. Phys. **80**, 997 (1993).
[75]Y. Sheng and A. Z. Panagiotopoulos, Macromolecules **27**, 400 (1994).
[76]L. G. MacDowell and F. J. Blas, J. Chem. Phys. **131**, 074705 (2009).
[77]A. Yethiraj and C. K. Hall, J. Chem. Phys. **96**, 797 (1992).
[78]J. K. Johnson, J. A. Zollweg, and K. E. Gubbins, Mol. Phys. **78**, 591 (1993).
[79]R. A. Reis, M. L. L. Paredes, M. Castier, and F. W. Tavares, Fluid Phase Equilib. **259**, 123 (2007).
[80]F. J. Blas, A. Ignacio Moreno-Ventas Bravo, J. M. Míguez, M. M. Piñeiro, and L. G. MacDowell, J. Chem. Phys. **137**, 084706 (2012).
[81]F. J. Blas, A. I. Moreno-Ventas Bravo, J. Algaba, F. J. Martínez-Ruiz, and L. G. MacDowell, J. Chem. Phys. **140**, 114705 (2014).
[82]G. A. Chapela and J. Alejandre, J. Chem. Phys. **135**, 084126 (2011).
[83]G. A. Chapela, E. Díaz-Herrera, J. C. Armas-Pérez, and J. Quintana-H, J. Chem. Phys. **138**, 224509 (2013).
[84]M. G. Martin and J. I. Siepmann, J. Phys. Chem. B **102**, 2569 (1998).
[85]M. N. Rosenbluth and A. W. Rosenbluth, J. Chem. Phys. **23**, 356 (1955).
[86]D. Frenkel and B. Smit, Mol. Phys. **75**, 983 (1992).
[87]D. Frenkel, G. C. A. M. Mooij, and B. Smit, J. Phys.: Condens. Matter **4**, 3053 (1992).
[88]A. Yethiraj and C. K. Hall, Mol. Phys. **72**, 619 (1991).